

# Method and Experiment of Fabricating and Cutting the Burr for Y Shape Nanochannel

Zone-Ching Lin, Hao-Yuan Jheng, Shih-Hung Ma

**Abstract**—The present paper proposes using atomic force microscopy (AFM) and the concept of specific down force energy (SDFE) to establish a method for fabricating and cutting the burr for Y shape nanochannel on silicon (Si) substrate. For fabricating Y shape nanochannel, it first makes the experimental cutting path planning for fabricating Y shape nanochannel until the fifth cutting layer. Using the constant down force by AFM and SDFE theory and following the experimental cutting path planning, the cutting depth and width of each pass of Y shape nanochannel can be predicted by simulation. The paper plans the path for cutting the burr at the edge of Y shape nanochannel. Then, it carries out cutting the burr along the Y nanochannel edge by using a smaller down force. The height of standing burr at the edge is required to be below the set value of 0.54 nm. The results of simulation and experiment of fabricating and cutting the burr for Y shape nanochannel is further compared.

**Keywords**—Atomic force microscopy, nanochannel, specific down force energy, Y shape, burr, silicon.

## I. INTRODUCTION

IN 2010, Hwang et al. [1] used laser beam machining to perform machining of a deep hole in conic pattern, and compared the output power between cone-free deep hole and conic deep hole. In recent years, related scholars have proved that AFM can be used to conduct surface machining of nano/microstructure. However, the substrate pattern machining mentioned in the above references all belong to micrometer machining. The paper innovatively proposes using AFM directly to perform the patternization of groove to be nanoscale pattern on Si substrate. AFM, invented by Bining et al. in 1986 [2], is a kind of scanning probe microscopy (SPM) generally used for measuring and observing the surface pattern of conductor and non-conductor. Therefore, related scholars made discussions on measurement and application of AFM. Additionally, for nanoscale microstructure machining, besides the high-cost electronic beam or ion beam machining methods, AFM also has been applied to nanolithography and nanoscale cutting. Application of AFM probe as a machining tool to carry out mechanical cutting has been proved by related scholars as a very useful technique in machining of nano/microstructure on the surface of semiconductor, photoelectric component, and metal [3]. Fang et al. [4] used AFM probe to conduct nanoscratch experiment of Si chip without coating of crystalline aluminum (Al) film. Experimental results showed that scratch depth deepened with

the increase of the load and scribing cycles of probe, with effects of down press normal force from tool being most obvious, and multi-pass machining deepened the depth of the cut groove with the increase of scratch cycles. Schumacher et al. [5] used AFM to conduct mechanical lithography on the surface of GaAs/AlGaAs hetero structure, and a single-electron transistor was machined. Yan et al. [6] directly used AFM to construct a system similar to CNC machining system, and undergo scratching of nano/microstructure on the surface of Si chip coated with copper film by AFM probe. Wang et al. [7] used AFM to perform machining of nanochannel on Si oxide surface, and conducted experiment to study how normal force is related to cutting speed and cutting depth. The paper refers to the micrometer channels in different shapes mentioned in [8], [9], which were T, Y, U, and orthogonal shapes. However, unlike this paper, the above references did not apply AFM and SDFE theory to undergo cutting of nanochannels in Y shape.

## II. EXPERIMENTAL SET-UP OF NANOCUTTING

The paper uses AFM apparatus to carry out nanoscale cutting, and measure the surface morphology of Y shape nanochannel before and after cutting. The paper takes Si substrate as the material of nanocutting experiment. The AFM apparatus used is a multimode AFM called Dimension 3100 produced by Veeco Instruments Inc.. The experiment uses a diamond-coated DT-NCHR AFM probe produced by Nanosensors company as the cutting tool of probe. The normal spring constant  $K_r$  of the probe is 60.8 N/m. It uses the force-distance curve to obtain  $d$  which is the offset amount of cantilever of probe with impact of normal down force. When multiplying the distance  $d$  by normal spring coefficient  $K_r$  of probe, down force  $F_d$  can be obtained as follows [10]:

$$F_d = k_r d \quad (1)$$

## III. USING SDFE THEORY TO ESTABLISH A FABRICATION MODEL OF Y SHAPE NANOCHANNEL AT A FIXED DOWN FORCE

Y shape is a very commonly seen nanochannel shape. The experiment used AFM apparatus to carry out simultaneously X-Y axial movement and plan a Y shape experimental path. First of all, a cutting pass was fabricated from the upper left part to the lower right part on the 1<sup>st</sup> cutting layer (the 1<sup>st</sup> cutting pass on the 1<sup>st</sup> cutting layer). Then, the offset was made downwards to the initial cutting position of vertical pass on the first cutting layer, and a vertical cutting pass was made from bottom to top on the 1<sup>st</sup> cutting layer, and connected to the cutting pass from the lower left part to the upper right part

Zone-Ching Lin, Hao-Yuan Jheng, and Shih-Hung Ma are with the Department of Mechanical Engineering, National Taiwan University of Science and Technology, Taiwan (e-mail: zclin@mail.ntust.edu.tw, M9903231@mail.ntust.edu.tw, M10303138@mail.ntust.edu.tw).

(the 3<sup>rd</sup> cutting pass on the 1<sup>st</sup> cutting layer). After cutting of the 3<sup>rd</sup> pass was completed, the probe offset leftwards and went back to the initial cutting position of the 1<sup>st</sup> cutting pass, and repeated the cutting path on the 2<sup>nd</sup> cutting layer. After such a repeated fabrication at a fixed down force by using SDFE theory, multi-layer cycled Y shape fabrication pass was completed, achieving the required depth and width. Fig. 1 shows the experimental path planning of cutting pass when carrying out fabrication cycle of Y shape nanochannel up to the 5<sup>th</sup> cutting layer.

#### IV. SIMULATION OF FABRICATING Y SHAPE NANOCHANNEL

The 1<sup>st</sup> cutting pass was firstly simulated on the 1<sup>st</sup> cutting layer. Offset was made downwards to the initial cutting position of vertical cutting pass on the 1<sup>st</sup> cutting layer, as shown in Fig. 2. A vertical cutting pass was made from bottom to top on the 1<sup>st</sup> cutting layer, and connected to the 3<sup>rd</sup> cutting pass on the 1<sup>st</sup> cutting layer, as shown in Fig. 3. After cutting of the 3<sup>rd</sup> cutting pass on the 1<sup>st</sup> cutting layer was completed, the probe offset leftwards and went back to the initial fabricating position of the 1<sup>st</sup> cutting pass, and repeated the same cutting path as the 1<sup>st</sup> cutting layer. Then, the simulation of cutting pass for multi-layer cycled cutting of Y shape nanochannel was completed.

#### V. SDFE THEORETICAL MODEL AND CALCULATION METHOD OF SDFE

The paper applies the definition of SDFE developed by author, in which the down force of the cutting tool of probe applied on workpiece is multiplied by the energy produced from the power of down press depth; and then the product is divided by the volume removed from Si workpiece by the down force of cutting tool. The value of SDFE equation is expressed as follows [10]:

$$\text{SDFE} = \frac{F_d \times \Delta d_n}{\Delta V_n} \quad (2)$$

where  $F_d$  is the down force applied on workpiece by cutting tool;  $\Delta d_n$  is the depth increment during the  $n$ th cutting pass; and  $\Delta V_n$  is the volume removed by down force on workpiece during the  $n$ th cutting pass. Since the volume removed from workpiece by down force changes with the increase of cutting depth,  $\Delta V_n$  is the function of cutting depth  $\Delta d_n$ . The paper uses the cutting depth measured in the cutting experiment by AFM at different down forces during the 1<sup>st</sup> cutting pass of straight-line cutting, the volume removed at such cutting depth calculated by CAD software, and SDFE concept for calculation, the results are shown in Table I. It is found that the SDFE tends to be a constant  $0.01775 \mu\text{N} \cdot \text{nm} / \text{nm}^3$ . The

paper carries out single-pass multi-layer cutting again at down force  $45.20 \mu\text{N}$ , to conduct cutting at experimental cutting depth for 5 passes and find the SDFE values. It is found that the average SDFE of the 5 cutting passes is around

$0.01775 \mu\text{N} \cdot \text{nm} / \text{nm}^3$ . Therefore, the paper lets the SDFE of Si substrate be  $0.01775 \mu\text{N} \cdot \text{nm} / \text{nm}^3$ . Using the concept that SDFE is a constant value, the paper establishes a new fabrication method of Y shape nanochannel on Si substrate.

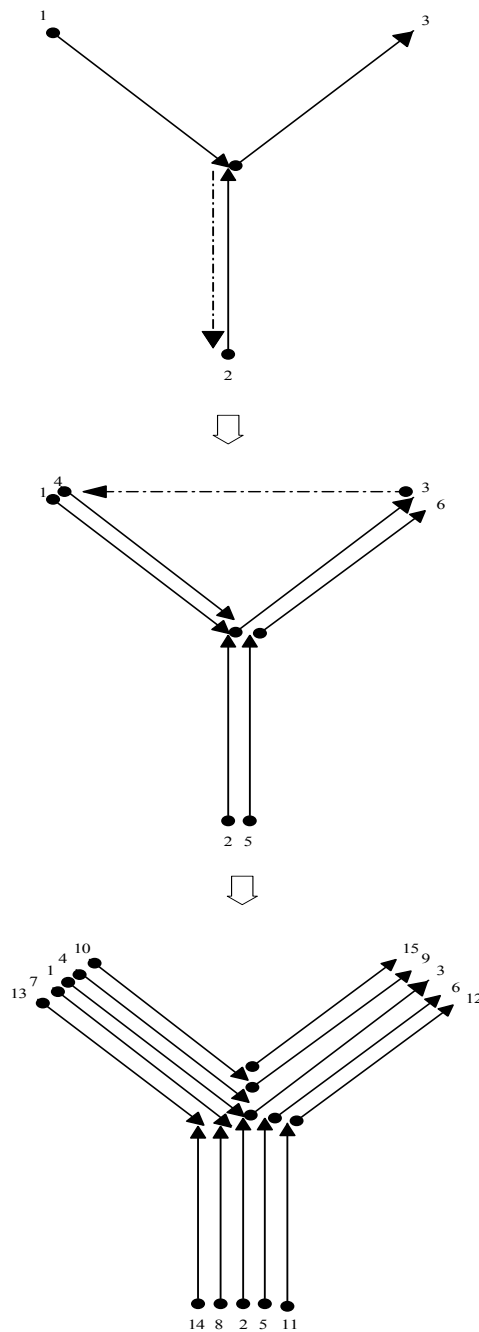


Fig. 1 Experimental path planning of cutting pass when carrying out fabrication cycle of Y shape nanochannel up to the 5<sup>th</sup> cutting layer

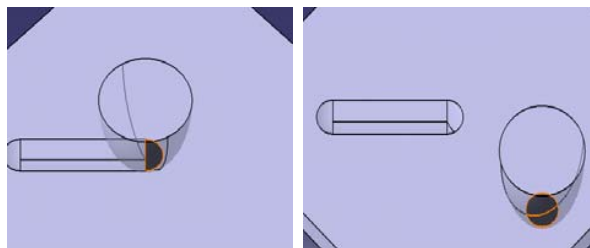


Fig. 2 After completing leftward offset cutting of Y shape at the 1<sup>st</sup> cutting pass on the 1<sup>st</sup> cutting layer, fabrication was simulated by the cutting tool which offset to the initial vertical cutting position of the 2<sup>nd</sup> cutting pass on the 1<sup>st</sup> cutting layer

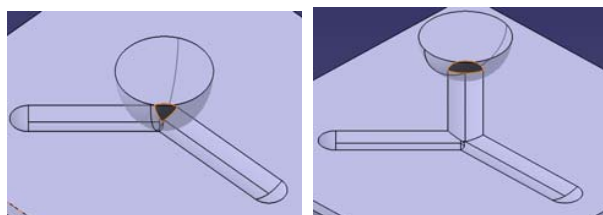


Fig. 3 After completing vertical cutting pass of Y shape on the 1<sup>st</sup> cutting layer, fabrication of rightward offset cutting of the 3<sup>rd</sup> cutting pass on the 1<sup>st</sup> cutting layer was simulated

TABLE I  
RELATED DATA OF THE 1<sup>ST</sup> CUTTING PASS OF STRAIGHT-LINE CUTTING AT  
DIFFERENT DOWN FORCE

Down force( $\mu\text{N}$ )	Cutting depth of the 1st pass measured in experiment (nm)	Removed volume of material calculated by CAD ( $\text{nm}^3$ )	SDFE value calculated by theoretical equation ( $\mu\text{N} \cdot \text{nm} / \text{nm}^3$ )
30.23	7.353	12524.63	0.01775
35.22	8.582	17013.96	0.01776
40.21	9.833	22272.45	0.01775
45.20	11.071	28154.41	0.01777

#### VI. ANALYSIS OF Y SHAPE NANOCANNEL EXPERIMENT

Figs. 4-6 show respectively the cutting depths and open widths of the nanochannels of the vertical cutting pass, and the leftward offset and rightward offset cutting passes on the 5<sup>th</sup> cutting layer after applying AFM to complete the cutting experiment of Y shape nanochannel on the 5<sup>th</sup> cutting layer. As seen from Figs. 4-6, the cutting depths and open widths of vertical cutting pass, and the leftward offset and rightward offset cutting passes on the 5<sup>th</sup> cutting layer have very similar values.

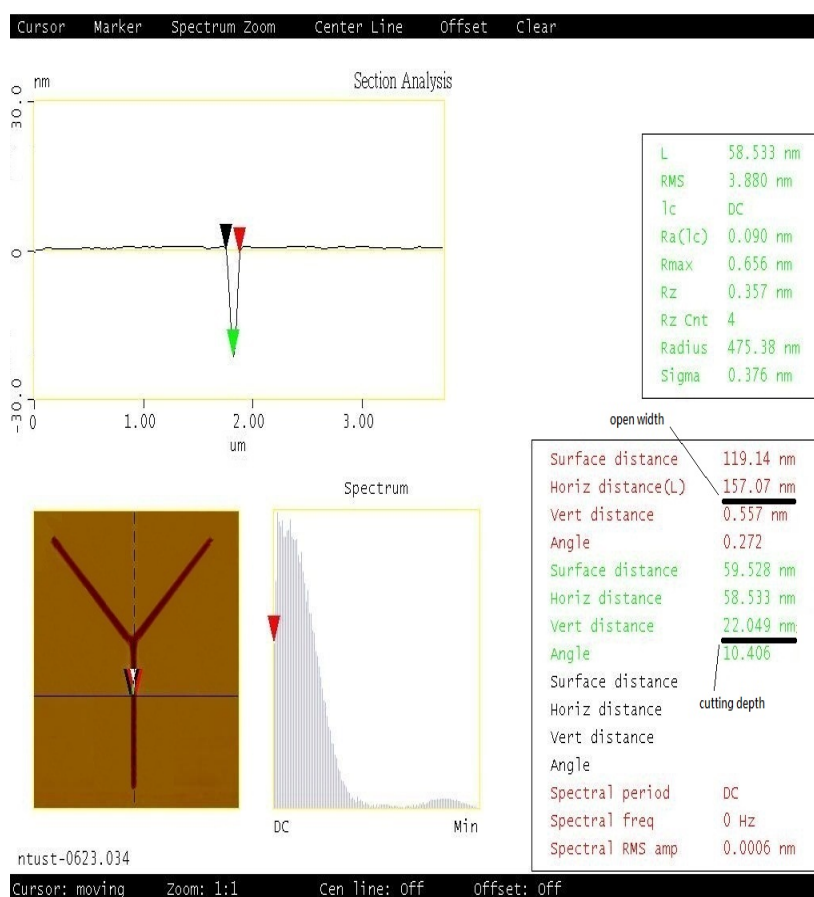


Fig. 4 Measurements of experimental results of vertical cutting pass' groove of Y shape nanochannel on the 5<sup>th</sup> cutting layer

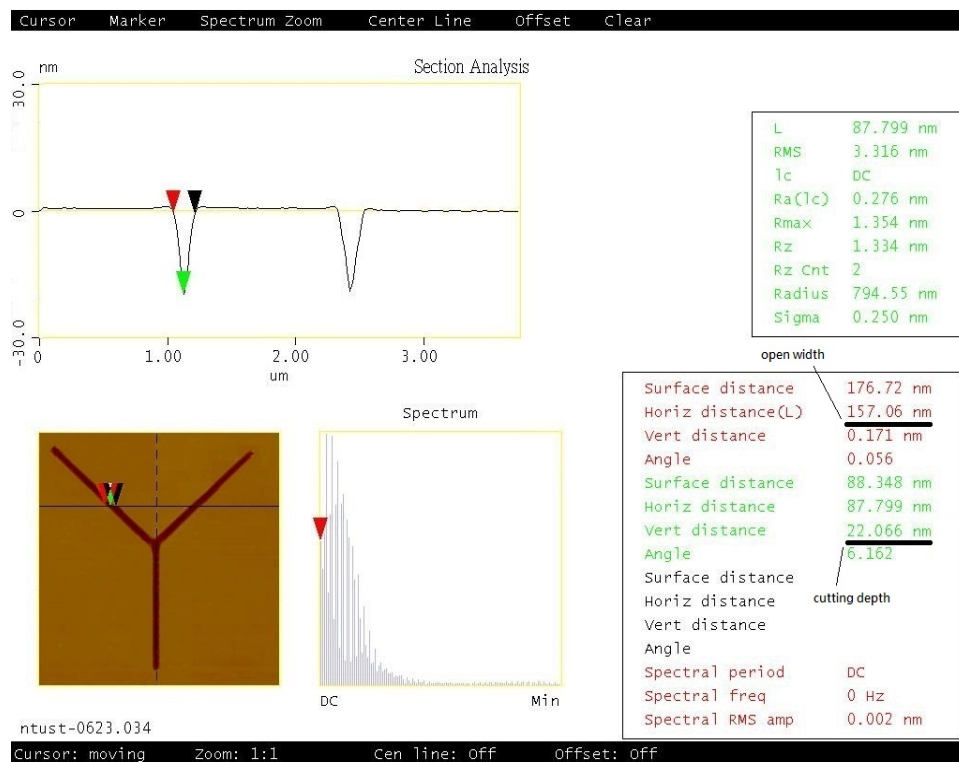
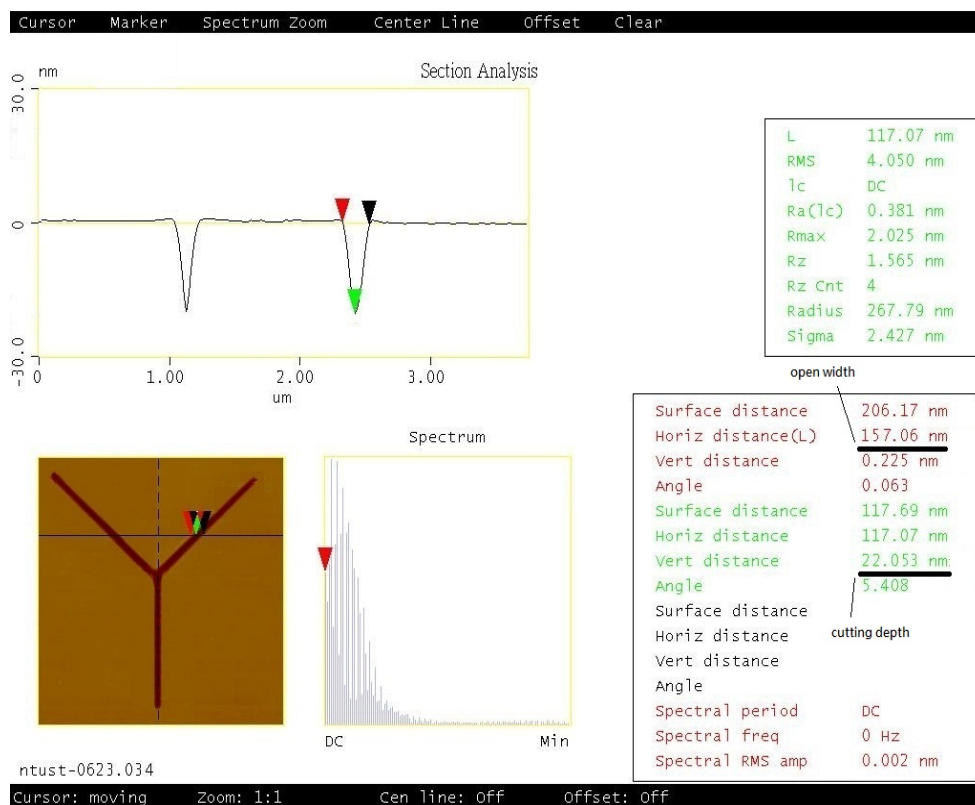
Fig. 5 Measurements of experimental results of leftward offset cutting pass' groove of Y shape nanochannel on the 5<sup>th</sup> cutting layerFig. 6 Measurements of experimental results of rightward offset cutting pass' groove of Y shape nanochannel on the 5<sup>th</sup> cutting layer

TABLE II  
COMPARISON BETWEEN EXPERIMENTAL AND SIMULATION RESULTS OF GROOVE'S CUTTING DEPTH AND GROOVE OPENING'S WIDTH OF Y SHAPE NANOCHANNEL FABRICATED ON THE 5<sup>th</sup> CUTTING LAYER AT DOWN FORCE 45.20 mN

Cutting pass	Measured cutting depth of nanochannel in experiment (nm)	Simulated cutting depth of nanochannel (nm)	Measured open width of nanochannel in experiment (nm)	Simulated open width of nanochannel (nm)	Experimental result of SDFE value ( $\mu\text{N} \cdot \text{nm} / \text{nm}^3$ )	Simulation result of SDFE value ( $\mu\text{N} \cdot \text{nm} / \text{nm}^3$ )
Vertical cutting pass	22.049	22.086	157.07	156.69	0.017756	0.017751
Leftward offset cutting pass	22.066	22.086	157.06	156.69	0.017759	0.017751
Rightward offset cutting pass	22.053	22.086	157.06	156.69	0.017759	0.017751

Table III indicates the difference between experimental results and simulation results shown in Table II. As seen from the comparative results in Tables II and III, the numerical experimental results and the numerical simulation results of the cutting depth, open width and SDFE value of Y shape nanochannel are quite similar. As to the percentage of difference, the greatest difference for cutting depth and open width is about 0.242%. Therefore, it is proved to be feasible to employ the way developed by the paper that AFM probe is used to fabricate Y shape nanochannel groove on single-crystal silicon substrate at a fixed down force.

TABLE III  
DIFFERENCE BETWEEN EXPERIMENTAL RESULTS AND SIMULATION RESULTS OF CUTTING DEPTH AND OPEN WIDTH

Cutting pass	Difference between experimental cutting depth and simulated cutting depth on the 5 <sup>th</sup> cutting layer (%)	Difference between experimental open width and simulated open width on the 5 <sup>th</sup> cutting layer (%)
Vertical cutting pass	0.168	0.242
Leftward offset cutting pass	0.115	0.236
Rightward offset cutting pass	0.149	0.236

## VII. PLANNING PATHS OF Y NANOCHANNEL EDGE FOR CUTTING THE BURR

As mentioned above, after completion of simulated fabricating of Y nanochannel, a starting point is set. According to the size of Y nanochannel edge acquired from the above simulation, the paper plans the path for cutting the burr at the edge, as shown in Fig. 7. Then, after using a smaller down force, it carries out cutting the burr along the Y nanochannel edge, and makes the height of standing burr at the edge maintaining at below the set value of 0.54 nm.

## VIII. ANALYSIS ON EXPERIMENTAL RESULTS OF BURR CUTTING OF CROSS-SHAPE NANOCHANNEL EDGE

Figs. 8 and 9 show the heights of standing burrs at the edge for vertical cutting pass and leftward offset cutting pass, respectively when fabricating Y shape nanochannel up to the 5<sup>th</sup> cutting layer without cutting the burr at the edge. The heights of standing burr at the edge maintain at the range of 1.159~1.610 nm.

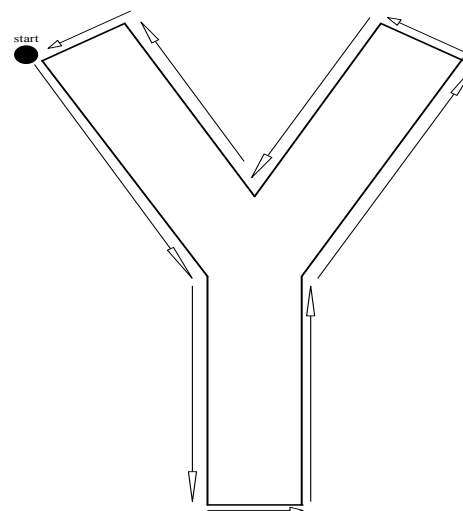


Fig. 7 Planning cutting paths for cutting the burr on the Y nanochannel edge

Figs. 10 and 11 show that after cutting the burr of Y nanochannel edge up to the 5<sup>th</sup> cutting layer at a set down force 5  $\mu\text{N}$ , the heights of standing burrs for vertical cutting pass and leftward offset cutting pass are both within the range of 0.507~0.521 nm. Therefore, the heights of standing burrs at the edges can reach the set convergence value of 0.54 nm.

## IX. CONCLUSION

The paper innovatively proposes and develops the fabricating method of Y shape nanochannel on single-crystal silicon substrate using the concept of SDFE and AFM apparatus. It proves that this method is feasible through experiment and simulation. Therefore, the paper simulates planning of cutting paths for fabricating Y shape nanochannel up to the 5<sup>th</sup> cutting layer, and the size of Y shape nanochannel edge after cutting up to the 5<sup>th</sup> cutting layer. The paper applies the self-developed method of cutting the burr of Y shape nanochannel edge at a smaller down force. Furthermore, the paper analyzes the cutting depth and open width of cutting Y shape nanochannel, and the height of standing burr at the edge. After cutting the burr at the edge, the height of standing burr at the edge of Y shape nanochannel edge would converge at below the set value.

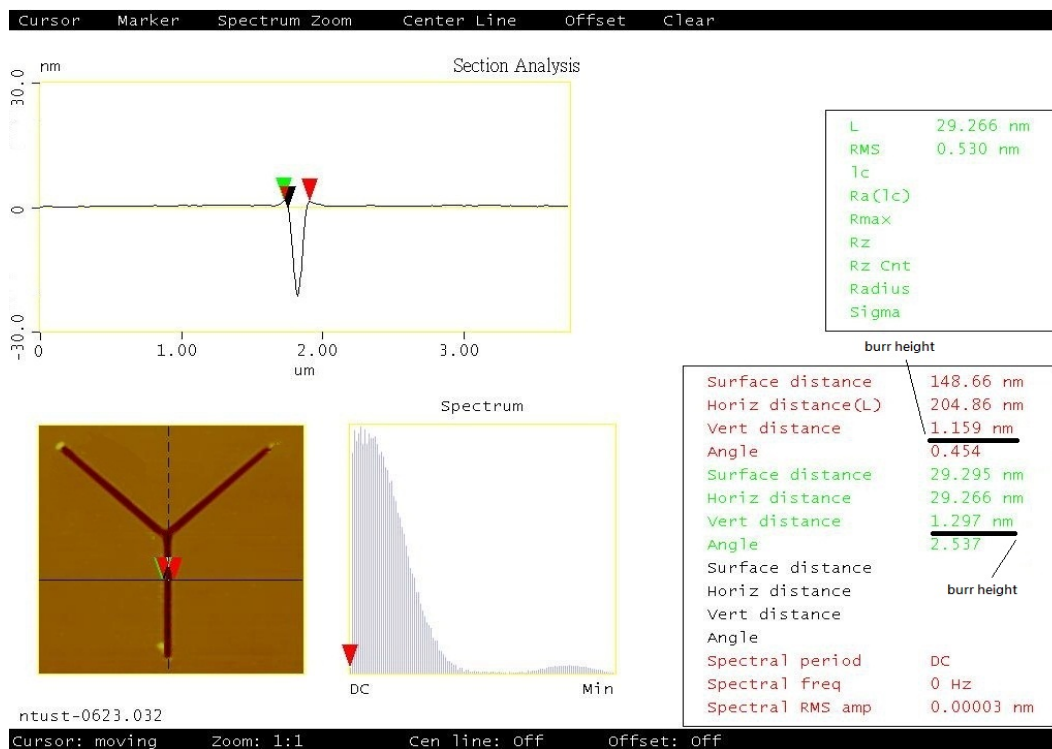


Fig. 8 Experimental measurement of the height of standing burrs at vertical cutting pass when fabricating Y shape nanochannel up to the 5<sup>th</sup> cutting layer

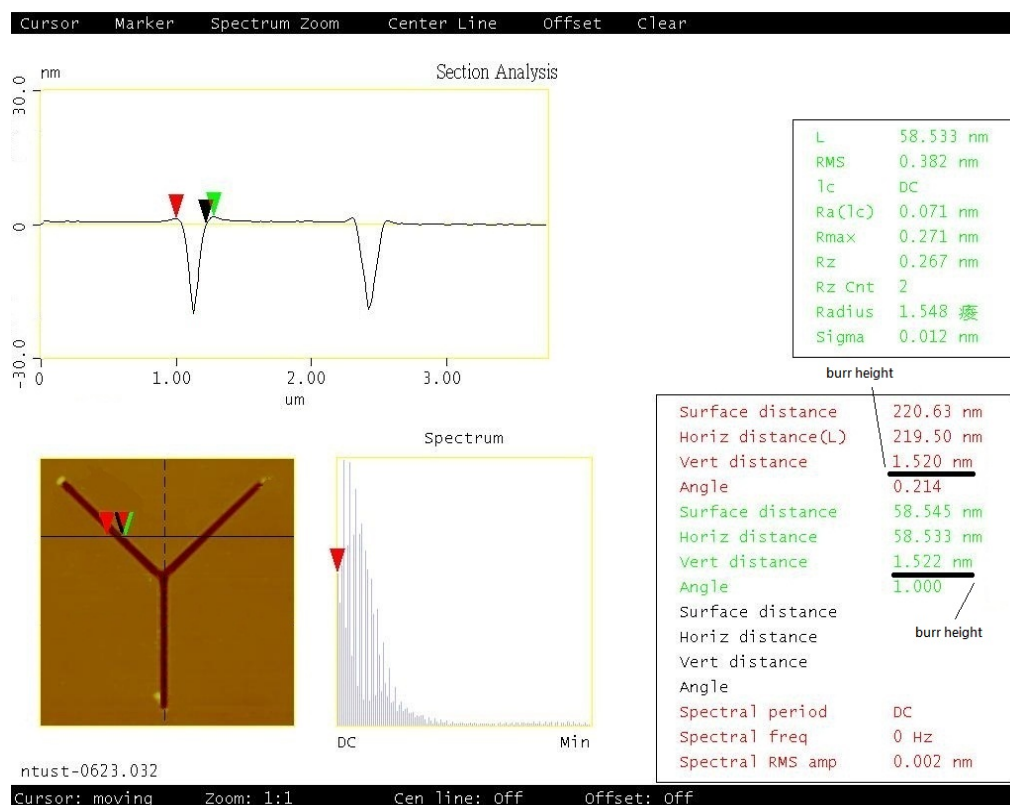


Fig. 9 Experimental measurement of the height of standing burrs at leftward offset cutting pass when fabricating Y shape nanochannel up to the 5<sup>th</sup> cutting layer

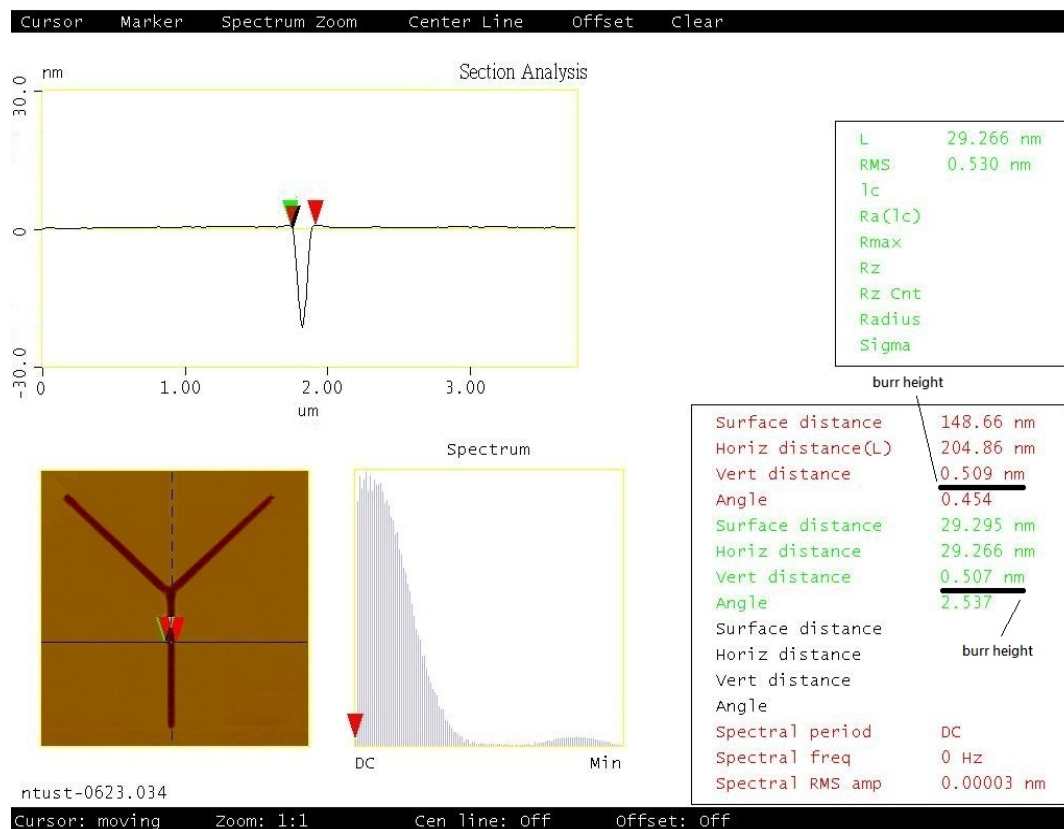


Fig. 10 Experimental measurement of the height of standing burrs at vertical cutting pass when fabricating Y shape nanochannel up to the 5<sup>th</sup> cutting layer

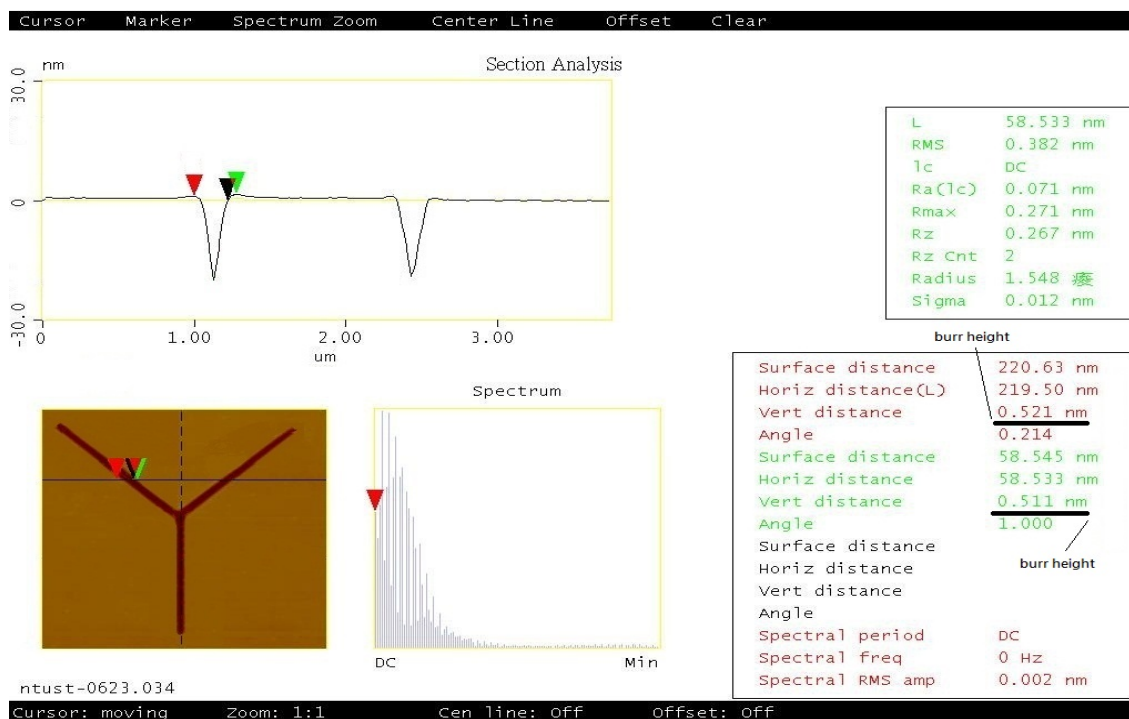


Fig. 11 Experimental measurement of the height of standing burrs at leftward offset cutting pass when fabricating Y shape nanochannel up to the 5<sup>th</sup> cutting layer



#### ACKNOWLEDGMENT

The authors would like to thank the support from Minster of science and technology, Taiwan. (MOST 104-2221-E-011-002)

#### REFERENCES

- [1] S.M. Hwang, N.S. Kim and J.H. Lee, IEEE Electron Device Letters, vol.31, 2010, pp. 698-700.
- [2] G. Binning, C.F. Quate and C. Gerber, Physical Review Letters, vol.56, 1986, pp. 930-933.
- [3] A.A. Tseng, S. Jou, A. Notargiacomo and T.P. Chen, Journal of Nanoscience and Nanotechnology, vol.8, 2008, pp. 2167-2186.
- [4] T.H. Fang, C.I. Weng and J.G. Chang, Nanotechnology, vol.11, 2000, pp. 181-187.
- [5] H.W. Schumacher, U.F. Keyser and U. Zeitler, Fabrication of a single-electron transistor, Physical. vol.6, 2000, pp. 860-863.
- [6] Y. Yan, T. Sun, Y.C. Liang and S. Dong, International Journal of Machine Tools and Manufacture, vol.47, 2007, pp. 1651-1659.
- [7] Z.Q. Wang, N.D. Jiao, S. Tung and Z.L. Dong, Chinese Science Bulletin, vol.55, 2010, pp. 3466-3471.
- [8] J.C.T. Eijkel, W. Sparreboom, L. Shui, G.B. Salieb-Beugelaar, and A. van den Berg, Nanofluidics: fundamentals and applications, vol.978, 2009, pp. 4193-4244.
- [9] L.L. Shui, C.T. Jan Eijkel and A. van den Berg, Sensors and Actuators B, vol.121, 2007, pp. 263-276.
- [10] Z.C. Lin, Y.C. Hsu, Applied Surface Science, vol.258, 2012, pp. 4513-4522.